JMSAE Journal of Materials Science and Applied Energy

Journal of Materials Science and Applied Energy

Journal home page: jmsae.snru.ac.th

Structural and Morphology of Hydrothermally Grown ZnO Nanorods on Zinc Sheets Towards 3D-Hybrid SERS Applications

Pacharamon Somboonsaksri[a], Saksorn Limwichean[b], Sukon Kalasung[b], Pennapa Muthitamongkol[c], Viyapol Patthanasettakul[b], Mati Horprathum[b], Noppadon Nuntawong[b], Pitak Eiamchai[b], Wantana Koetniyom[a, *]

[a] *Department of Industrial Physics and Medical Instrumentation, Faculty of Applied Science, King Mongkut's University of Technology North Bangkok, Bangkok,10800 Thailand*

[b] *National Electronics and Computer Technology Center (NECTEC), National Science and Technology Development Agency, Pathum Thani, 12120 Thailand*

[c] *National Metal and materials Technology Center (MTEC), National Science and Technology Development Agency, Pathum Thani, 12120 Thailand*

*Corresponding Author: wantana.k@sci.kmutnb.ac.th

Received 4 August 2020; **Revised** 24 August 2020; **Accepted** 3 December 2020; **Available online:** 1 January 2021

Abstract

This research studies the fabrication of surface-enhanced Raman spectroscopy (SERS) substrate with self-cleaning effect and can be reusability. Start with the preparation of zinc oxide on the zinc sheet with the hydrothermal process by observing the effects of time to grow crystals of zinc oxide nanorods with hexagonal structures. In the experiment, we studied the characteristics of ZnO nanorod structures depending on precursors of zinc nitrate ($Zn(NO_3)_2$) : hexamethylentetramine (HMTA) at 1:1 ratio, in DI water at concentration of 10 mM by varying growth time at 4 – 10 h. The prepared zinc oxide templates were finally decorated with gold (Au) nanoparticles with the sputtering deposition technique for 90 seconds. From physical observations was investigated by the field emission scanning electron microscopic (FE-SEM) showed the length of ZnO nanorods was increased from 774 – 1660 nm corresponding with the growth time increased. After Au decoration ZnO nanorods were characterized by transmission electron microscopy (TEM). The prepared SERS substrates were finally measured for the Raman enhancement by Handheld Raman spectroscopy with Rhodamine 6G (R6G) as the test molecules and test reusability efficiency. The growth time of hydrothermal at 6 h shows that the high performance of enhanced Raman signal and minimum cleaning time is 10 minutes. The results show that the SERS substrates can be detected the R6G solution at the limit of detection of 1×10^{-6} M. In addition, the SERS substrates were tested reusability up to 10 cycles with the UV cleaning process.

Keywords: Zinc oxide; Surface Enhanced Raman Spectroscopy; Reusability; Hydrothermal process; Handheld Raman spectroscopy

Introduction

Raman spectroscopy is a technique used to observe vibrational, rotational, and frequency modes in a system [1] that is commonly used in chemistry to provide a fingerprint by which molecules can be identified. However, when some of substances have very low Raman signals, it is necessary to improve a surface that can enhance the Raman signals. Surface-enhanced Raman spectroscopy (SERS) has been developed by many researchers for several years towards high sensitivity in trace detection and to provide the enhanced Raman signals more than one million times [2]. Generally, SERS-active materials include noble metals such as Pt, Ag, Cu, and Au [3]. The Raman signal enhancement is a result of the photons of laser that stimulate free electrons at the surface of the metal. When molecules fall into the hot-spots on the metal surface, resonance which greatly enhances the occurrence of the Raman signals. This phenomenon is called a localized surface plasma resonance (LSPR) effect. From this effect, the SERS has been widely developed towards applications in forensic [4], medical [5], pharmaceutical, [6] and agricultural [7] fields of study. Most of the developed SERS-active nanostructures can be typically classified into three types: (1) colloidal, (2) thin film-based, and (3) 3D hybrid structures. The colloid-based SERS materials are usually noble metal nanoparticles in solution form, generally prepared by chemical processes such as Au-colloid solution prepared chemical synthesised [3, 29]. This type of the SERS materials is generally required multi-step preparation process and treatments of wasted chemicals. For the thin film-based SERS substrates are usually noble metal nanostructures prepared on a smooth surface. This type of the SERS substrates can be prepared from various techniques, for examples, chemical vapor deposition (CVD) and physical vapor deposition (PVD) such as Au-Ag dealloyed nanorod SERS by co-sputtering technique by oblique angle deposition (OAD) [8, 9, 28], to provide the high Raman signal enhancement. However, there are also limitations to the preparation process and cost-effectiveness. Finally, the 3D-hybrid nanostructures are recently developed based on first preparations of base materials for use as templates with the micro-nanometer scale, and then decorations of the noble metals by any methods.

Regardless of any types of the SERS nanostructures, the SERS substrates can only be used once and then discarded. To cope with high cost and production complications, many researchers are highly interested in development of the SERS substrates that can be reused again. Therefore, with the 3D-hybrid nanostructured approaches, semiconductor materials with photocatalytic properties [10] are used to fabricate templates that allow self-cleaning properties. This type of the SERS substrates would offer both excellent enhanced Raman signal and reusability one than more times by a simple UV exposure. The semiconductor materials that are commonly used include titanium dioxide (TiO_2), silicon dioxide (SiO_2), and zinc oxide (ZnO). Among these materials, ZnO exhibits unique characteristics over other materials with a wide band gap of 3.37 eV [10], is one of the multifunctional material a suit of useful properties, such as optical, transparent conductivity, sensitivity and photocatalysis [11]. In addition, ZnO nanostructures can be easily prepared by several methods, for examples, sol-gel spinning, CVD, precipitation, microemulsion, sonochemistry, and electrical coating [10]. One of the most popular methods is the hydrothermal process [12], which is easy to prepare at low cost and can be used to fabricate ZnO in the form of nanorod arrays. The research of ZnO nanorods arrays attracts the worldwide interests, because of their electrical and optical properties. In addition, It has been proposed that vertically grown ZnO nanorods may considerably increase the transfer of electrons thus effect to photocatalytic properties [11, 27]. ZnO is an interesting material to SERS fabrication with reusable properties

based on photocatalysis [11]. However, the hydrothermal process requires the ZnO seed layer to induce the charge between the surface of the zinc oxide film and the zinc ion inside the solution in order to form the zinc oxide nanostructures [13, 14]. We propose a method to reduce this step. To make the preparation process easier, the process will not requires seed layer by applying zinc sheet for preparation as a substrate for growing the zinc oxide nanostructure.

In this work, we therefore present a method to fabricate of the ZnO nanorod arrays based on the hydrothermal process on bare zinc sheets without any seed layer. Since the hydrothermal process conditions, i.e., growth time, growth temperature, and precursor concentration [12] can affect the ZnO nanostructures, this study would therefore focus on the hydrothermal growth time that affected the size, length, and spacing of the ZnO nanorod arrays. Finally, the prepared ZnO nanorod arrays were further decorated with gold nanoparticles. The obtained 3D hybrid SERS substrates were investigated toward the SERS performance and reusability, and finally discussed with respect to the ZnO nanorod template conditions.

Materials and Methods

Fabrication of the SERS Substrates

First, zinc oxide nanostructured templates were fabricated from Zn sheets (99.98 % purity) based on a hydrothermal process. The Zn sheets at 1.50 × 1.50 cm^2 in dimension and 0.50 mm thickness were used as a base material substrate. The hydrothermal process was performed using zinc nitrate ($Zn(NO_3)_2$) and hexamethylenetetramine (HMTA; $C_6H_{12}N_4$) at 1:1 ratio, mixed in DI water at 10 mM. The sample container was taken in the stainless steel autoclave, set at 90°C. The hydrothermal growth conditions were performed at 4, 6, 8, and 10 h. The obtained ZnO nanorod templates were then rinsed with DI water and heated in air ambience for 30 min [12, 15].

Next, the Au nanoparticles were decorated on the prepared ZnO nanorod templates by a magnetron sputtering technique (ATC 2000-F; AJA International). The sputtering process used Au target (95.50% – purity). The sputtering process, argon gas was generated at a flow rate of 20 sccm at operated pressure of 5, the power for sputtering was 100 W and deposition time of 90 s.

Characterization

The physical morphologies of the ZnO nanorod templates and the Au-decorated ZnO samples were characterized by field-emission scanning electron microscopy (FE-SEM; Hitachi S-8030), x-ray diffraction (XRD; Rigaku TTRAX III) and transmission electron microscopy (TEM; JEOL JEM 2010). The internal structures of the prepared samples ZnO were observed by Raman spectroscopy (inVia Raman microscope; Renishaw plc) with a 532 nm laser wavelength, 25 mW laser power, and 20 s accumulation time. The SERS performance of the samples was tested by handheld Raman spectroscopy (Mira DS Advanced; Metrohm AG). The Raman measurements were performed with 785 nm laser wavelength, 100 mW laser power, and 20 s accumulation time, based on Rhodamine 6G (R6G) at 1×10^{-5} M as test molecules. The limit of detection of the zinc oxide SERS substrates was tested with the R6G solution at $1 \times 10^{-3} – 1 \times 10^{-7}$ M. The reusable properties of the SERS samples were tested with the R6G solution, and alternately irradiated with an ultraviolet (UV) source for several cycles.

Results and Discussion

Figure 1 demonstrate the morphological analyses from the FE-SEM images of the prepared samples. Fig. 1(a) shows the physical morphologies of the ZnO nanorod templates, which indicates the hexagonal wurtzite structures of ZnO nanorods prepared at various hydrothermal growth times. Since the hydrothermal fabrications were performed with the 10 mM concentration, the ZnO nanorods were grown mainly along the c-axis direction. The ZnO nanorods were observed to correspond with the <0001> direction and growth along the <1000> direction [16]. The variations of the growth times affected not only the growth rate but also the growth direction. Fig. 1(a) also shows that the average dimensions, i.e., size and length, of the ZnO nanorods. As the hydrothermal growth time was increased, the nanorod size was increased from 52 to 92 nm, and the length was increased from 774 to 1660 nm. The changes in the nanorod dimensions would greatly affect the performance of the SERS substrates because of the changes in the hot spots from the decrease in number density of the nanorods, as shown in Fig. 1(b). Further FE-SEM analyses toward vertical alignments of the ZnO nanorods were shown in Fig. 1(c), where numbers densities were counted towards the nanorod angles from the substrate normal. The results clearly showed that the ZnO nanorod templates prepared at the hydrothermal growth time of 6 h yielded the highest orderly arrangements of the vertically aligned nanorod.

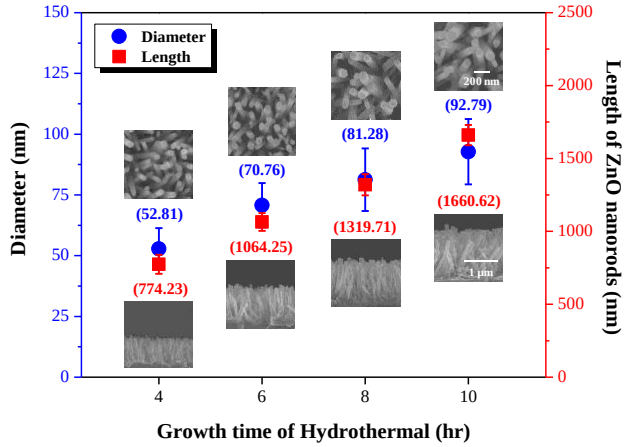

(a)

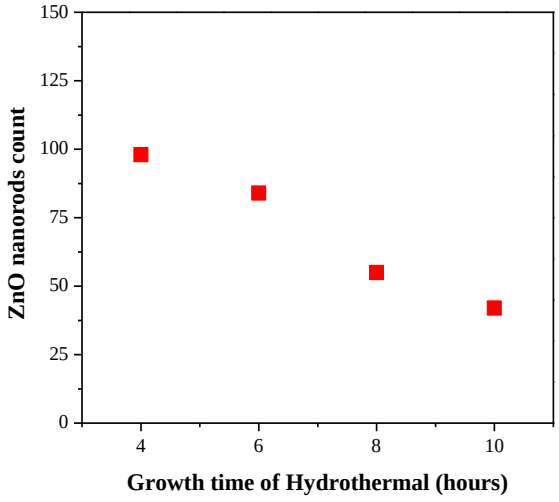

(b)

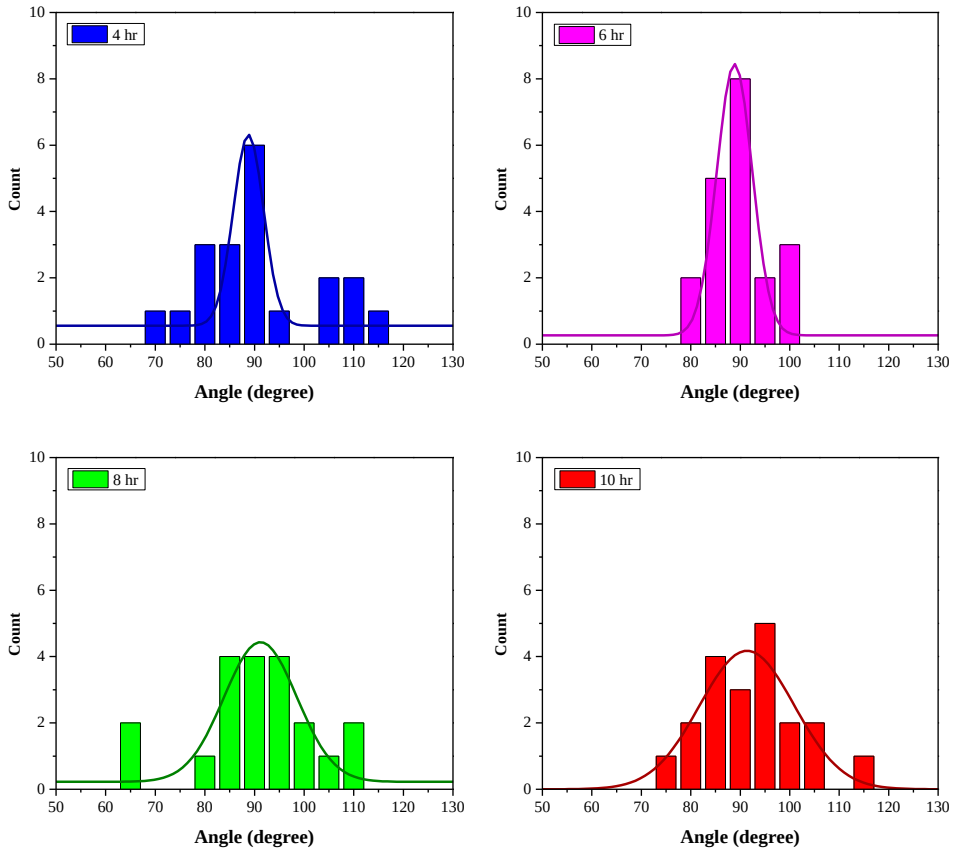

(c)

Fig. 1 (a) FE-SEM images and the calculated dimensions of the ZnO nanorods prepared at various hydrothermal growth time, (b) number density of ZnO nanorod in the observed FE-SEM imaging areas, and (c) number density of angle-variation of the prepared ZnO nanorods.

Figure 2 shows the Raman measurements of the ZnO nanorod arrays prepared at various growth time of hydrothermal. The results showed a dominant peak at 439 cm^{-1}, corresponding to the characteristic Raman active mode of the wurtzite hexagonal structure, and minor peaks at 332 and 379 cm^{-1} [11, 17], associated with the ZnO material. The figure also demonstrated that all hydrothermal growth time yielded the preferred ZnO crystalline structures. Fig. 2 (b) XRD pattern was confirmed the ZnO crystal structure, the XRD peaks corresponding to ZnO (002), (101) and (103) planes, which are located at 34.49°, 36.34°, and 62.89°, respectively [18, 19]. From Fig. 2 (b) indicated that shows the growth of ZnO nanorods, the increase growth time effect to crystallinity of ZnO nanorod. ZnO nanorods prepared from the growth time at 6 h show the highest intensity of crystallinity due to the arrangement, uniformity and vertically of ZnO nanorods.

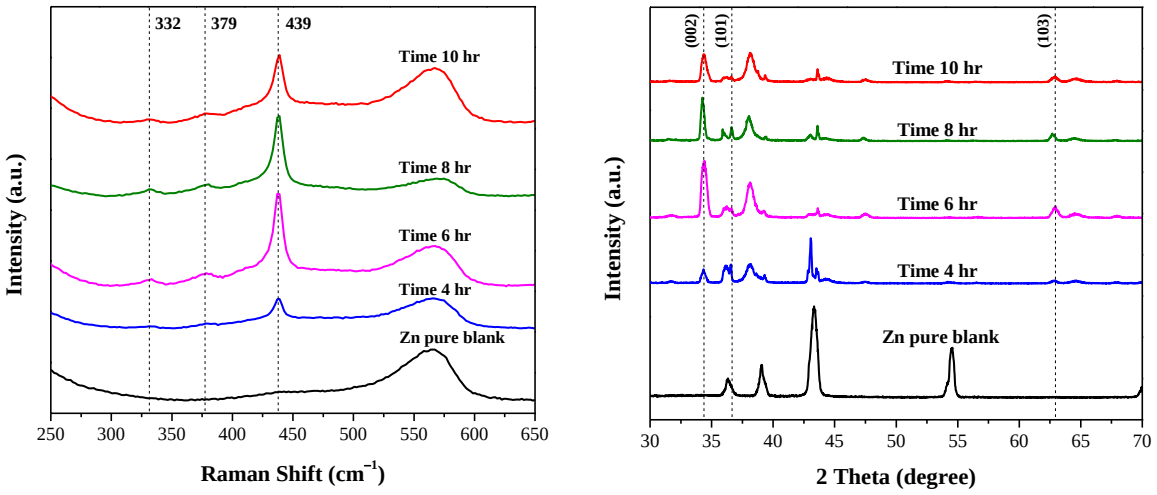

(a) (b)

Fig. 2 (a) Raman spectra of the ZnO nanorod arrays, hydrothermally grown on the Zn sheet substrates and (b) XRD patterns of ZnO nanorod prepared at various growth time of hydrothermal.

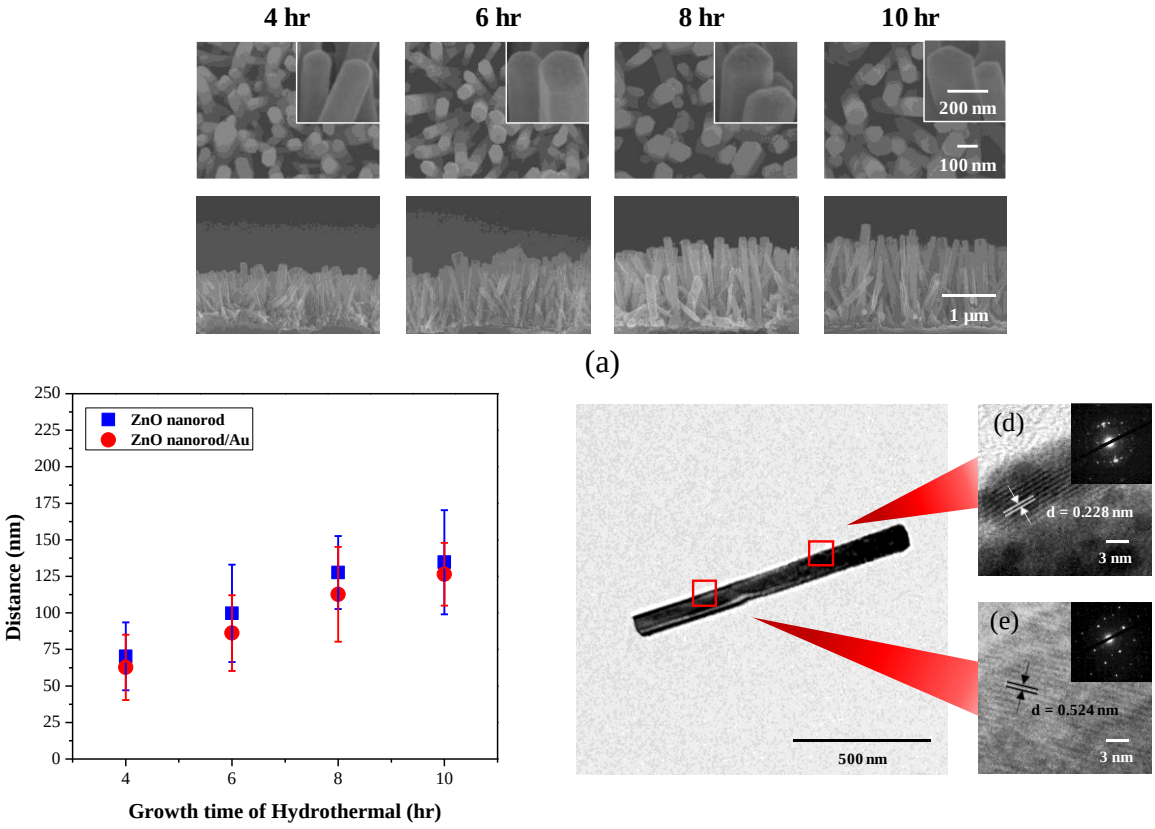

(a) (b) (c)

Fig. 3 (a) FE-SEM images of the Au-decorated ZnO nanorod arrays prepared at various hydrothermal growth times, (b) Determined distance of the as-prepared and the Au-decorated ZnO arrays, with respect to the hydrothermal growth time. (c) TEM image of a single Au-decorated ZnO nanorod at the 6 h hydrothermal growth time. The high-resolution TEM images represented lattice spacing for (d) the Au nanoparticle, and (e) the ZnO nanorod.

The obtained ZnO nanorod templates were then decorated with the Au nanoparticles. Fig. 3(a) demonstrated the FE-SEM images of the Au/ZnO SERS samples, which showed the gold nanoparticles covering the top surface of the ZnO nanorod arrays, and somewhat distributed in the bottom of the ZnO nanorods. Because the SERS performance generally depended on the shape and size of the noble metal nanoparticles with arbitrary hot spot spacing, Fig. 3(b) shows the measured distance between the nanorod at various growth time of hydrothermal process, both before and after the Au decorations. The results showed that the nanorod distances were nearly identical with their respective standard deviation falling in the same range. These results clearly indicated that the Au nanoparticle decorations had little effect towards the inter-nanorod distance. On the other hand, the increase in the hydrothermal growth time directly affected the increased nanorod distance. Further investigations from the TEM micrographs, as shown in Fig. 3(c), showed the Au nanoparticles on ZnO nanorod surface. The HR-TEM image analyses on the ZnO nanorods also confirmed the wurtzite structure. The resultant lattice spacing of 5.24 Å indicated the occurrence of the (001) planes, respectively. In addition, the lattice spacing of 2.28 Å also corresponding to the d-spacing of (111) Au crystal plane [20].

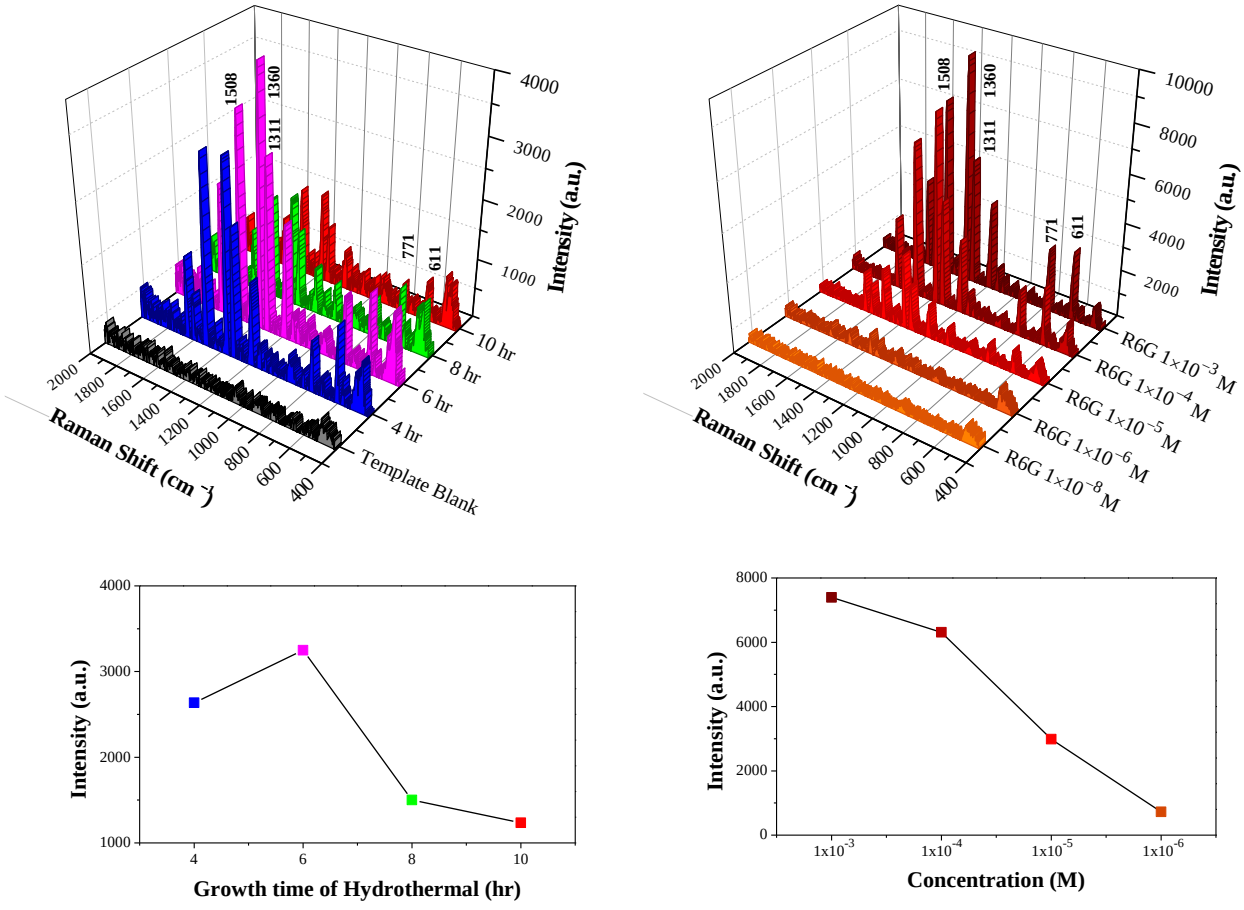

(a) (b)

Fig. 4 (a) Raman spectral results of the R6G test molecules with respect to different preparation conditions of the ZnO SERS substrates, (b) R6G solution concentrations, (c) and (d) Subset plots demonstrated the highest Raman intensities at 1360 cm^{-1} for each sample conditions.

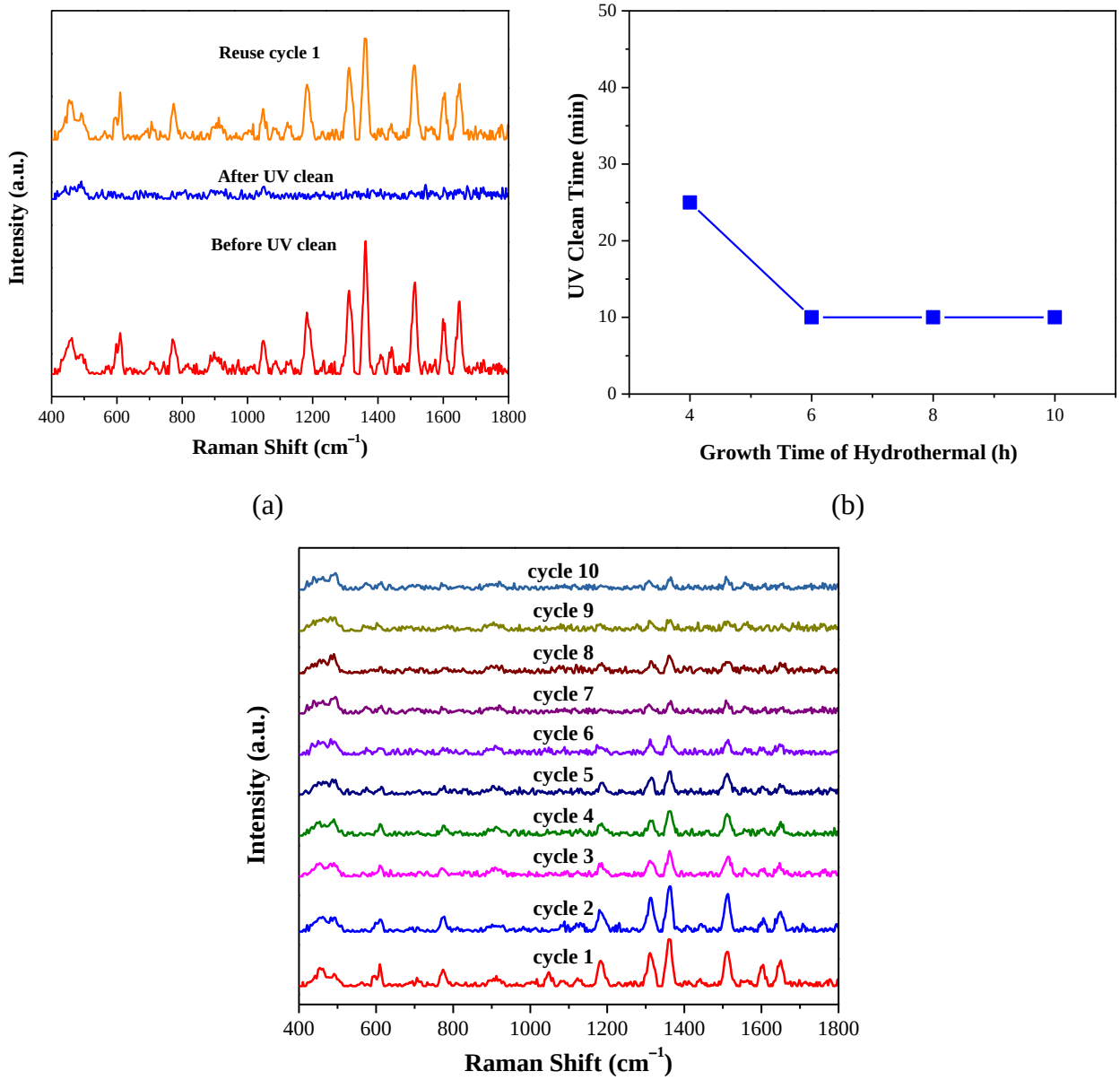

Fig. 5 (a) Raman spectra for one cycle of reusability of the Au/ZnO SERS samples as tested by 1 × 10^{-5} M R6G solution, (b) UV-cleaning time of the Au/ZnO SERS samples prepared at different hydrothermal conditions, and (c) Raman spectra of the Au/ZnO SERS sample hydrothermally prepared at 6 h were tested with the R6G solution up to 10 cycles.

The performance of the prepared ZnO SERS substrates was investigated with the R6G as the test molecules. Fig. 4(a) shows that the SERS Raman signals of R6G at concentration 1 × 10^{-5} M dropped on the Au-decorated ZnO nanorods, which has been prepared at different growth times during the hydrothermal process. The results showed dominant peaks at 611, 771, 1311, 1360 and 1508 cm^{-1}, which can be assigned as (C–C) ring, (C–H) out-of-plane bending, (C–H) bending, (C–C) stretching and (C–C) stretching, respectively [17, 21]. It can be seen that the samples with 6 h growth time demonstrated the highest Raman intensity. According to the results from Fig. 1, the optimal diameter and distance of the ZnO nanorods were reported at 70 and 86 nm, respectively, and were most suitable towards the Raman enhancement. Therefore, the SERS

templates prepared from the hydrothermal growth time at 6 h were further investigated for limit of detection (LOD) from the R6G solution, with varying concentrations from $1 \times 10^{-3} – 1 \times 10^{-7}$ M. Fig. 4(b) showed that the prepared SERS substrates clearly offered the limit of detection down to 1×10^{-6} M of the R6G molecules.

For the reusable performance of the SERS samples, The R6G solution at 10^{-5} M was used as the test molecules, and the UV irradiation was used to clean the molecules on SERS surface by the photocatalytic process. For each cycle of Raman measurements, the R6G solution was dropped on the SERS surface. The Raman spectra were collected (1) before the UV exposure, (2) after the UV exposure, and (3) after another drop of R6G. Fig. 5(a) showed an example of the Raman spectral results from one cycle of using the ZnO SERS samples. With each cycle of reusable process, all the prepared SERS samples were examined toward the most optimized UV-cleaning time. Fig. 5(b) shows that the Au/ZnO SERS samples prepared at 6, 8, and 10 h offered the fastest UV-cleaning time within 10 minutes. This result clearly showed that at 6 h or more of the hydrothermal growth, the ZnO nanorod templates offered excellent self-cleaning properties without degrading effect toward the reusability. Therefore, the Au/ZnO SERS samples prepared at 6 h hydrothermal process were finally tested, where Fig. 5(c) indicated that this SERS sample allowed the reusability up to 10 cycles. The Raman signal was decrease from cycle 1 to cycle 10 due to Au/ZnO SERS under UV light irradiation during photocatalytic reactions effect to the electrons changes on surface Au nanoparticles. It produces the negative effect of Au LSPR and only some electrons on Au nanoparticles take partin the LSPR effect. Therefore, the efficiency of Raman enhancement was decrease and shows the low signal of R6G [22, 23].

In comparison to previously published studies, as shown in Table 1, our experimental results demonstrated that our approaches toward the fabrications of the ZnO nanorod templates were straightforward without having to prepare the ZnO seed layer prior to the hydrothermal process. This method was therefore simple and inexpensive to prepare highly consistent ZnO nanorod arrays with small variation in dimension and length. In addition, the ZnO nanostructures show to have the highly uniform and vertically aligned nanorod arrays that were best suitable toward development of high performance SERS substrates with additional reusable properties.

Table 1 Summary of resultant ZnO nanostructured templates prepared by the hydrothermal process toward different applications.

Substrate	Seed	Method	Diameter (nm)	Application	Ref.
Si	ZnO seed-layer	Hydrothermal 6 h	61 – 73	SERS Sensors	[15]
Bare Si,	–	Hydrothermal 8 h	~ 300	Photonics device	[24]
Bare Cu,	–				
Si	ZnO seed-layer				
FTO	ZnO nanoseed	Hydrothermal 8 h	90 ± 15	DSSC	[25]
Zn foil	–	Hydrothermal 12 h	50 – 200	Remediation of AZO-dye effluents	[26]
Zn sheet	–	Hydrothermal 6 h	52 – 92	SERS Sensors	(This work)

Conclusion

We have successfully prepared 3D-hybrid SERS from zinc sheets as templates by a simple process and cost-effective. Preparing ZnO nanostructures on the zinc sheets with the hydrothermal process by varying times to grow crystals of zinc oxide nanorods with the hexagonal wurtzite structures was carried. The results show that the diameter and length of zinc oxide nanorods were increased follow with growth time and also effected to enhancement of Raman signal. The optimized growth time of hydrothermal process at 6 h due to vertically alignments of ZnO nanorods and uniformity of structure which shows the highest Raman signals that tested by Rhodamine 6G molecules. ZnO SERS presents the detection limit in the range of $1 \times 10^{-3} – 1 \times 10^{-6}$ M. The SERS reusability performance by UV cleaning uses 10 min and can be reusability up to at least 10 cycles.

Acknowledgement

For our success in this research, we would like to thank Opto-Electrochemical Sensing Research Team (OEC), National Electronics and Computer Technology Center (NECTEC), National Metal and materials Technology Center (MTEC), National Science and Technology Development Agency (NSTDA), the place for this research and for the uses of the instrument.

References

[1] J.J. Bohning, T. N. Misra, M. Choudhury, The Raman Effect, American Chemical Society, Calcutta, 1998.

[2] M. Fleischmann, P.J. Hendra, A.J. McQuillan, Raman spectra of pyridine adsorbed at a silver electrode, Chem. Phys. Lett. 26 (1974) 163 – 166.

[3] R. Pilot, R. Signorini, C. Durante, L. Orian, M. Bhamidipati, L. Fabris, Review on Surface-Enhanced Raman Scattering, Biosensors. 9 (2019).

[4] A. Hakonena, K. Wu, M.S. Schmidt, P.O. Andersson, A. Boisen, T. Rindzevicius, Detecting forensic substances using commercially available SERS substrates and handheld Raman spectrometers, Talanta. 189 (2018) 649 – 652.

[5] E. Prado, A. Colin, L. Servant, S. Lecomte, SERS spectra of oligonucleotides as fingerprints to detect label-free RNA in microfluidic devices, J. Phys. Chem. C. 118 (2014) 13965 – 13971.

[6] H. Mao, M. Qi, Y. Zhou, X. Huang, L. Zhang, Y. Jin, Y. Penga, S. Du, Discrimination of sibutramine and its analogues based on surface-enhanced Raman spectroscopy and chemometrics: toward the rapid detection of synthetic anorexic drugs in natural slimming products, RSC Adv. 5 (2014) 5886 – 5894.

[7] S. Kreisig, A. Tarazona, E. Koglin, The adsorption of paraquat on silver electrode surfaces: a SERS microprobe study, Electrochim. Acta. 42 (1997) 3335 – 3344.

[8] R.F. Bunshah, Deposition technologies for films and coatings: developments and applications, Noyes Publications, 1982.

[9] J.E. Mahan, Physical vapor deposition of thin films, Wiley-VCH, Colorado, 2000.

[10] X. Ren, D. Han, D. Chen, F. Tang, Large-scale synthesis of hexagonal cone-shaped ZnO nanoparticles with a simple route and their application to photocatalytic degradation, Mater. Res. Bull. 42 (2007) 807 – 813.

[11] J. Yanga, J. Zhenga, H. Zhai, X. Yang, L. Yang, Y. Liu, J. Lang, M. Gao, Oriented growth of ZnO nanostructures on different substrates via a hydrothermal method, J. Alloys Compd. 489 (2010) 51 – 55.

[12] W. Koetniyom, P. Somboonsaksri, J. Prasobchokchaikun, S. Kalasung, N. Nuntawong, V. Patthasettakul, M. Horprathum, S. Limwichean, P. Eiamchai, Reusability of SERS-Active surfaces based on Gold-decorated hexagonal ZnO nanorod used zinc sheet as template, Surf. Rev. Lett. 25(Supp01) (2018) 1840004.

[13] S. Baruah, J. Dutta, Hydrothermal growth of ZnO nanostructures, Sci. Technol. Adv. Mater. 10 (2009) 013001.

[14] J. Song, S. Lim, Effect of Seed Layer on the Growth of ZnO Nanorods, J. Phys. Chem. C. 111 (2007) 596 – 600.

[15] S. Kalasung, C. Chananonnawathorn, M. Horprathum, P. Thongpanit, P. Eiamchai, S. Limwichean, N. Pattanaboonmee, N. Witit-anun, K. Aiempanakit, Low-Temperature Synthesis of Nanocrystalline ZnO Nanorods Arrays, J. Adv. Mater. Res. 770 (2013) 237 – 240.

[16] M. F. Mele´ndrez, K. Hanks, Francis Leonard-Deepak, F. Solis-Pomar, E. Martinez-Guerra, E. Pe´rez-Tijerina, M. Jose´-Yacaman, Growth of aligned ZnO nanorods on transparent electrodes by hybrid methods, J. Mater. Sci. 47(4) (2012) 2025 – 2032.

[17] H. Watanabe, N. Hayazawa, Y. Inouye, S. Kawata, DFT Vibrational Calculations of Rhodamine 6G Adsorbed on Silver: Analysis of Tip-Enhanced Raman Spectroscopy, J. Phys. Chem. B. 109 (2005) 5012 – 5020.

[18] S. Kim, M. C. Jeong, B. Y. Oh, W. Lee, J. Myoung ,Fabrication of Zn/ZnO nanocables through thermal oxidation of Zn nanowires grown by RF magnetron sputtering, J. Cryst. Growth. 290 (2006) 485 – 489.

[19] W. Muhammad, N. Ullah, M. Haroon, B. H. Abbasi, Optical, morphological and biological analysis of zinc oxide nanoparticles (ZnO NPs) using Papaver somniferum L, RSC. Adv. 9 (2019) 29541 – 29548.

[20] J. Wu, C. Tseng, Photocatalytic properties of nc-Au/ZnO nanorod composites, Appl. Catal. 66 (2006) 51 – 57.

[21] M. Tran, A. Fallatah, A. Whale, S. Padalkar, Utilization of Inexpensive Carbon-Based Substrates as Platforms for Sensing, Sensors. 18 (2018) 2444.

[22] J. Prakasha, S. Sunc, H. C. Swart, R. K. Guptaa, Noble metals-TiO2 nanocomposites: From fundamental mechanisms to photocatalysis, surface enhanced Raman scattering and antibacterial applications, App. Mat. 11 (2018) 82 – 135.

[23] Y. Chenga, W. Wanga, L. Yaob, J. Wangc, H. Hana, T. Zhua,Y. Lianga, J. Fua, Y. Wanga, 3D Ag/ZnO microsphere SERS substrate with ultra-sensitive, recyclable and self-cleaning performances: application for rapid in site monitoring catalytic dye degradation and insight into the mechanism, Colloids. Surf., A Physicochem. Eng. Asp. 607 (2020) 125507.

[24] L.L. Yang, J. H. Yang, D. D. Wang, Y. Zhanga, Y. Wanga, H. Liua, H. Fana, J. Langa, Photoluminescence and Raman analysis of ZnO nanowires deposited on Si (100) via vapor-liquid-solid process, Physica E Low Dimens. Syst. Nanostruct. 40 (2008) 920 – 923.

[25] I. Iwantono, W. Nurwidya, L.R. Lestari, F.Y. Naumar, S. Nafisah, A.A. Umar, M.Y.A. Rahman, M.M. Salleh, Effect of growth temperature and time on the ZnO film

properties and the performance of dye-sensitized solar cell (DSSC), J. Solid. State Electrochem. 19 (2015) 1217 – 1221.

[26] X. Cai, B. Han, S. Deng, Y. Wang, C, Dong, Y. Wang, I. Djerdj, Hydrothermal growth of ZnO nanorods on Zn substrates and their application in degradation of azo dyes under ambient conditions, Cryst. Eng. Comm. 16 (2014) 7761 – 7770.

[27] S.V. Nipane, P.V. Korake, G.S. Gokavi, Graphene-zinc oxide Nanorod nanocomposite as photocatalyst for Enhanced degradation of Dyes under UV light irradiation, Ceram. Int. 41(3) (2014) 4549 – 4557.

[28] U. Waiwijit, C. Chananonnawathorn, P. Eimchai, T. Bora, G.L.Hornyak, N. Nuntawong, Fabrication of Au-Ag SERS substrates by co-sputtering technique and dealloying with selective chemical etching, Appl. Surf. Sci. 530 (2020) 147171.

[29] S.E.J. Bell, M.R. McCourt, SERS enhancement by aggregated Au colloids: effect of particle size, Phys. Chem. Chem. Phys. 11 (2009) 7455 – 7462.